ISTITUTO NAZIONALE DI RICERCA METROLOGICA
Repository Istituzionale

Self-compensating networks for four terminal-pair
impedance definition in current comparator bridges

Terms of use:

(Article begins on next page)

03 May 2024

Self-compensating networks for four terminal-pair impedance definition in current comparator bridges

Luca Callegaro, Vincenzo D'Elia, Jan Kučera, Massimo Ortolano, Faranak Pourdanesh, and Bruno Trinchera

Abstract—The four terminal-pair (4TP) definition of impedance standards allows to reach ultimate accuracy in impedance metrology. In general, the 4TP definition requires dedicated circuitry to be included in the bridge network and the attainment of auxiliary bridge balances during the measurement. A careful choice of the network topology allows the bridge to be *self-compensating*: the 4TP definition is in large part achieved by the behaviour of the network itself, without any adjustment. The additional circuitry required for impedance definition can therefore be simpler, the balancing procedure becomes easier, and a more robust 4TP can be achieved. This paper analyses a current comparator bridge network with a topology featuring self-compensation. A digitally-assisted test bridge has been implemented; test measurements on ac resistance comparison in the $25\,\Omega$ to $100\,\Omega$ range, at kHz frequency, are reported.

Index Terms—Metrology, impedance measurement, admittance measurement, measurement standards, bridge circuits.

I. INTRODUCTION

Primary impedance metrology widely employs coaxial transformer ratio bridges [1]–[3]: the impedance ratio to be measured is thus directly related to a voltage or current ratio, this being highly stable and very close to the transformer nominal turns ratio.

Most accurate current ratio bridges are based on the *current comparator* principle [4]–[7]. In an ideal current comparator with N primary windings, currents I_k ($k = 1, \ldots, N$) are linked by n_k turns to a ferromagnetic core with magnetic permeance $\mathcal{P}$. The core is thus energized by the magnetomotive force[1] $\mathcal{M} = \sum_{k=1}^{N} n_k I_k$ which generates the magnetic flux $\Phi = \mathcal{P}\mathcal{M}$. The comparator is provided with a detection winding to sense Φ. At equilibrium, when $\Phi = 0$, the condition $\mathcal{M} = 0$ holds true; in addition, the voltages across the windings are zero.

The schematic of a basic current comparator impedance bridge is shown in Fig. 1. The admittances under comparison are Y_A (impedance $Z_A = 1/Y_A$) and Y_B (impedance $Z_B = 1/Y_B$). These are assumed of the same type, so that their ratio is close to a real number. The two impedances are excited by the voltage source E and the bridge equilibrium is sensed by the detector D. At equilibrium, the currents through Y_A and Y_B are respectively $I_A = Y_A E$ and $I_B = Y_B E$; since $n_1 I_1 + n_2 I_2 = n_1 I_A - n_2 I_B = 0$, the admittance and impedance ratios are given by:

$$W = \frac{Z_A}{Z_B} = \frac{Y_B}{Y_A} = \frac{n_1}{n_2}. \tag{1}$$

In Fig. 1, Z_A and Z_B are defined as two-terminal impedances. Primary impedance measurements require, instead, more sophisticated impedance definitions, the most accurate of which is the *four terminal-pair* (4TP) definition [9].
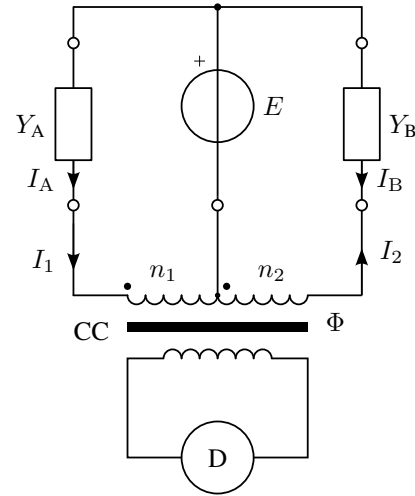

Fig. 1. Schematic of a basic current comparator bridge. Y_A and Y_B are the impedances under comparison, here defined as two-terminal standards; CC is the current comparator; E is the voltage source which provides the bridge excitation; and D is the detector which senses the bridge balance.

A proper 4TP definition of the impedances Z_A and Z_B can be achieved by several methods, employing either passive or active networks [3, Ch. 4.6.4]. In voltage ratio bridges, a typical solution is the use of *combining networks* [2, Ch. 5.6], realized with variable electromagnetic devices, possibly remotely controlled [10], [11].

Digitally-assisted bridges (see [3, Ch. 5.4.1] and references therein; [12]–[14]) aim to achieve the defining conditions by driving the bridge network with synthesized sinusoidal voltage or current sources. For example, a digitally-assisted four terminal-pair current comparator bridge, which employs a five-channel synthesized source, was recently built by the authors [12]. This bridge implements a fully active compensation

Luca Callegaro, Vincenzo D'Elia and Bruno Trinchera are with the Electromagnetism Division of the Istituto Nazionale di Ricerca Metrologica (INRIM), strada delle Cacce 91, 10135 Torino, Italy. E-mail: l.callegaro@inrim.it

Jan Kučera is with Czech Metrology Institute (ČMI), Prague, Czech Republic.

Massimo Ortolano and Faranak Pourdanesh are with the Politecnico di Torino, Torino, Italy, and INRIM.

Manuscript received September 29, 2015.

[1]In the following, turn numbers n_k shall be considered positive integer numbers; accordingly, currents shall be considered positive when entering into the terminals marked by a dot (dot convention [8]).

scheme: for each impedance, the voltage drop developed along the low-current path (the connections and the corresponding current comparator winding) is nulled with the injection of a countervoltage of the same amplitude and opposite phase. At low impedance values, this strategy requires demanding specifications on the source channel outputs, in particular in terms of output current capability and voltage stability. It was found experimentally that, given the properties of the source employed, the bridge is limited to an impedance range of $100\,\Omega$ or greater to achieve uncertainties of interest for primary metrology (below 10^{-5}).

Although better performing sources [15] can be employed to extend the measurement range to lower impedance magnitudes, it is also of interest to investigate alternative bridge topologies, which might require less demanding specifications on the sources employed to achieve the four terminal-pair definition of the standards.

In this paper we investigate experimentally the properties of a bridge topology proposed nearly 50 years ago by Moore and Basu [16]. Our implementation, introduced in [17], is here described in full detail with the measurement model and an evaluation of the uncertainty of the test measurements.

The bridge topology [16] employs a clever arrangement of electromagnetic devices (instrument transformers) to automatically achieve a first approximation of the four-terminal definition of the impedances under comparison, without the need of any active injection. Experiments have shown that, for impedances in the $10\,\Omega$ to $100\,\Omega$ range at kHz frequency, the approximation of the four-terminal definition is sufficient for primary metrology experiments without further refinements. The four-terminal definition is extended to a four terminal-pair definition with the help of a Wagner balance [18]. To extend the impedance range to lower values or to further improve the accuracy, adding less critical active compensations to this bridge topology is straightforward.

II. BRIDGE NETWORK AND MEASUREMENT MODEL

The schematic of the bridge is shown in Fig. 2. Potentials V_{AL}, V_{BL}, V_{AH} and V_{BH} are measured with respect to the ground defined by the bridge shield (see Sec. III-D). Three main electromagnetic devices are included: CC is the current comparator and is provided with three primary windings and a detection winding; CT is a current transformer; and VT is a double isolation transformer.

VT has the same primary-to-secondary ratio for both secondary windings and excites the bridge with the same voltage E on both arms.

Given two like impedances Z_A and Z_B with nominal values Z_A^{nom} and Z_B^{nom} and nominal ratio $W^{nom} = Z_A^{nom}/Z_B^{nom}$, the turn numbers n_1 and n_2 of CC and CT should be chosen to have a turns ratio $n_1/n_2 = W^{nom}$.

The third winding of CC, which interconnects the low-voltage terminals of Z_A and Z_B, should be set for a turn number $n_3 = n_1 + n_2$. At equilibrium, the magnetic flux Φ in CC is zero and, therefore, this winding acts as a low-impedance interconnection. If the condition $n_3 = n_1 + n_2$ is met, the current I_3 flowing through the interconnecting
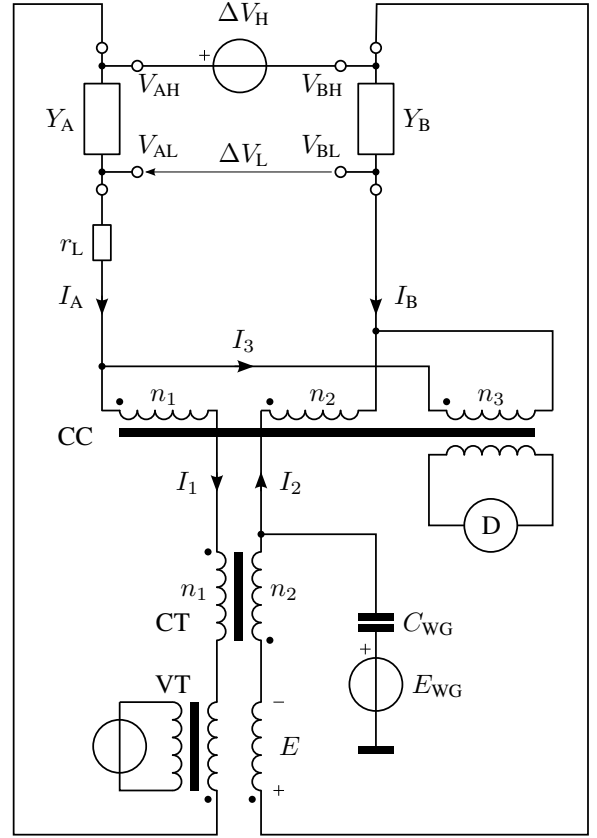

Fig. 2. Schematic of the current comparator bridge, in a non-coaxial representation. The admittances Y_A and Y_B being compared are defined as four-terminal standards. CC is the current comparator; D is the detector; CT is a current transformer which works as current equalizer; VT is a voltage transformer which provides the bridge excitation E to both arms; E_{WG} and C_{WG} form the Wagner arm circuit (see Sec. III-D); r_L is an additional resistor employed to check the effectivness of the self-compensating network.

winding does not enter in the equilibrium equation of CC. In fact,

$$0 = \sum_{n=1}^{3} n_k I_k = n_1(I_A - I_3) + n_2(-I_B - I_3) + n_3 I_3 , \quad (2)$$
$$= n_1 I_A - n_2 I_B . \quad (3)$$

Moreover, the current I_3 is virtually nulled by the action of CT, which works as a current equalizer [1, Ch. 1.6]. In fact, the voltages which develop across its windings are such to maintain the condition

$$n_1(I_A - I_3) - n_2(I_B + I_3) = 0 , \quad (4)$$

and since at equilibrium $n_1 I_A = n_2 I_B$ (Eq. (3)), we have $I_3 = 0$. In this way, the difference $\Delta V_L = V_{AL} - V_{BL}$ between the low potentials V_{AL} and V_{BL} of Z_A and Z_B is driven to zero (if parasitic parameters are neglected).

To summarize, at the equilibrium $\Delta V_L \approx 0$ because both $\Phi \approx 0$ and $I_3 \approx 0$. The effectiveness of this arrangement can be checked by adding a relatively high resistance r_L in series to the low-current path of one of the two impedances, as shown in Fig. 2.

The high-voltage terminals of Z_A and Z_B are interconnected through a low-impedance voltage source ΔV_H, which can be adjusted until the equilibrium of CC is attained.

The Wagner arm circuit is composed of the voltage source E_{WG} and the capacitor C_{WG}. The voltage phasor E_{WG} is adjusted in magnitude and phase to have $V_{BL} = 0$.

The measurement model can be derived as follows. From Fig. 2, applying the Kirchhoff's voltage law to the loop containing Z_A and Z_B yields

$$\Delta V_H + Z_B I_B - \Delta V_L - Z_A I_A = 0. \tag{5}$$

From the above and Eq. (3), we obtain

$$W = \frac{Z_A}{Z_B} = \frac{n_1}{n_2}\left(1 + \frac{\Delta V_H - \Delta V_L}{Z_B I_B}\right). \tag{6}$$

To account for the nonidealities of CC, the turns ratio can be written as

$$\frac{n_1}{n_2} = W^{\mathrm{nom}}(1 + \epsilon), \tag{7}$$

where ϵ, with $|\epsilon| \ll 1$, is potentially a non-zero, complex valued deviation from ideality. In addition, since $V_{BL} \approx 0$, it is $Z_B I_B \approx V_{BH}$. Eq. (6) can thus be rewritten as (second-order error terms have been neglected)

$$W = W^{\mathrm{nom}}\left(1 + \epsilon + \frac{\Delta V_H - \Delta V_L}{V_{BH}}\right). \tag{8}$$

The measurement model of Eq. (8) is valid for generically complex quantities. However, since all the standards compared in this paper are resistors with small time constants, in the following we shall consider only the real part of W. We can therefore define

$$\delta = \mathrm{Re}\,\frac{W - W^{\mathrm{nom}}}{W^{\mathrm{nom}}}, \tag{9}$$

and write the measurement model in the following form:

$$\delta = \mathrm{Re}\left[\epsilon + \frac{\Delta V_H - \Delta V_L}{V_{BH}}\right], \tag{10}$$

$$= \mathrm{Re}\,\epsilon + \frac{\mathrm{Re}\,\Delta V_H - \mathrm{Re}\,\Delta V_L}{V_{BH}}, \tag{11}$$

where in the last equation we assumed that V_{BH} is real, that is, that the phases of ΔV_H and ΔV_L are measured with respect to V_{BH}.

III. IMPLEMENTATION

The schematic of Fig. 2 was tested with the electromagnetic devices and the digital source already employed in [12]. A photograph of the set-up is shown in Fig. 3.

A. Digital sources

The bridge is excited with a polyphase DDS generator, already described in other works [19], [20]. The core of the generator is a commercial digital-to-analogue (DAC) board[2]. The board is programmed for a continuous generation of sine waves; each wave can be updated without stopping the

---

[2]National Instruments mod. NI PCI-6733: 8 DAC outputs, variable reference input, 16 bit resolution, maximum sampling rate $1\,\mathrm{MS}\ \mathrm{s}^{-1}$, voltage span $\pm 10\,\mathrm{V}$.
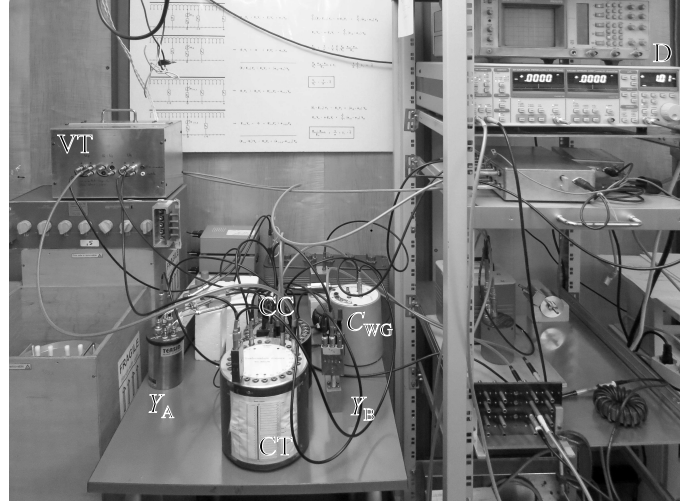

Fig. 3. Photograph of the bridge set-up.

generation, thereby avoiding harmful voltage steps in the electromagnetic components.

Three DAC channels are employed. The DAC outputs are cascaded to $30\,\mathrm{kHz}$ two-pole low-pass Butterworth filters to reduce the quantization noise and to buffer amplifiers with automatic control of the dc offset [21].

B. Current comparator

The comparator, described in [12], is realized on a nanocrystalline toroidal ferromagnetic core. From inner to outer, the core is wound with a 200-turn detection winding, magnetic and electrostatic shields, and the main ratio windings (10×10 turns each). Consistency checks performed on different winding sections permit to establish a maximum deviation of the current comparator ratio from the ideal turns ratio $|\epsilon| < 10^{-6}$ at $1\,\mathrm{kHz}$ frequency.

C. Other bridge components

CT is a shielded current transformer with two identical windings on a Supermalloy core. Each winding has 10×10 turns, hence allowing to set the same $n_1 : n_2$ ratio of CC.

The voltage source ΔV_H is realized with a $200 : 1$ injection transformer connected to one of the channels of the digital source. The step-down injection transformer is employed to have finer steps in the adjustment of ΔV_H.

Bridge balance is detected by a commercial synchronous detector (Stanford Research Systems mod. 830 lock-in amplifier), connected in sequence to different detection points. The equilibrium is semi-automated: after the detector is manually connected to a detection point, a balancing routine [22] adjusts the corresponding generator until the magnitude of the detected signal decreases below a given threshold.

D. Coaxial bridge

The schematic of Fig. 2 was realized with fully coaxial standards and connections. A coaxial schematic of the current comparator bridge is shown in Fig. 4. Coaxial equalizers were employed to achieve a proper coaxial condition [3, Sec. 3.5.2].
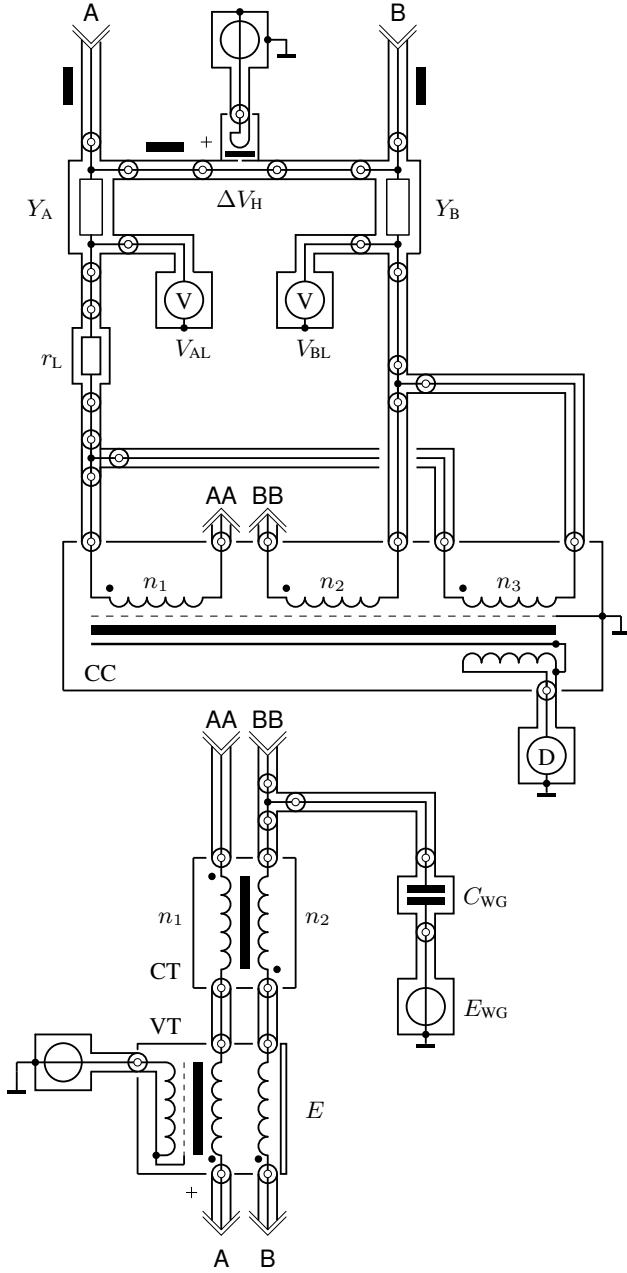
Fig. 4. Coaxial schematic of the current comparator bridge. The three coaxial equalizers are denoted by thick black rectangles.

E. Measurement procedure

The measurement procedure is the following:

1) Zeroing of V_{BL} by adjustment of E_{WG}.
2) Main bridge balance: zeroing of D by adjustment of ΔV_H.
3) Iteration of steps 1 and 2. Typically three or four iterations are sufficient to achieve convergence.
4) Measurement of V_{AL} with the synchronous detector; evaluation of $\Delta V_L = V_{AL} - V_{BL} \approx V_{AL}$.
5) Measurement of V_{BH} with the synchronous detector.

The typical time for the first reading is about $10\,\mathrm{min}$. The measurement time can be reduced by employing an automated coaxial switch to connect the synchronous detector to the

different detection points [23].

IV. EXPERIMENTAL

The measurements were mainly focused on the demonstration of the self-compensation functionality of the proposed bridge topology, and on the evaluation of its effectiveness for different values of the lead resistances. These changes were physically simulated by connecting an additional resistance box r_L in series with the lead path from the Y_A low-current terminal pair to the corresponding CC input. The resistance r_L was varied from about $0\,\Omega$ to $10\,\Omega$: this upper limit, largely exceeding the impedance of a typical bridge connection lead, was deliberately chosen to stress the bridge self-compensation mechanism.

The standards chosen for the measurements are listed in Tab. I. All measurements were performed at a frequency of $1541\,\mathrm{Hz}$.

Tab. II reports the results of the measurements performed. The columns report the following information:

- The standards employed as Z_A and Z_B. Refer to Tab. I for a description;
- The nominal resistance ratio $W^{\mathrm{nom}} = R_A^{\mathrm{nom}}/R_B^{\mathrm{nom}}$;
- The reference ratio deviation $\delta^{\mathrm{ref}} = (W^{\mathrm{ref}} - W^{\mathrm{nom}})/W^{\mathrm{nom}}$, where W^{ref} is a low-frequency reference ratio determined with two independent ratio measurement: one, a dc four terminal measurement, was made with an Agilent mod. 3458A in ratio mode; the other was made with a commercial transformer ratio bridge (Automatic Systems Laboratories F18 precision thermometry bridge) operating at $25\,\mathrm{Hz}$ and $75\,\mathrm{Hz}$. The frequency dependence of the $25\,\Omega$ resistor is specified to be lower than 10^{-6} for frequencies up to $1592\,\mathrm{Hz}$. The other standards ($100\,\Omega$ and $*100\,\Omega$) were characterized in frequency by substitution comparison with a Tinsley mod. 5685A $100\,\Omega$ ac-dc standard, also specified for an ac-dc dependence lower than 10^{-6}.
- The ratio deviation $\delta^0 = (W^0 - W^{\mathrm{nom}})/W^{\mathrm{nom}}$ measured with the current comparator bridge in the unperturbed condition, that is, with $r_L \approx 0\,\Omega$;
- The ratio deviation δ^L, defined as δ^0 above but with $r_L = 10\,\Omega$, corresponding to a simulated increase of the lead resistance of $10\,\%$ of Z_A for $W^{\mathrm{nom}} = 1$ and of $40\,\%$ for $W^{\mathrm{nom}} = 0.25$. When r_L is switched from $0\,\Omega$ to $10\,\Omega$, the bridge unbalance is about 3×10^{-5} when $W^{\mathrm{nom}} = 1$ and 7×10^{-5} when $W^{\mathrm{nom}} = 0.25$. The value of δ^L reported here is the result obtained after rebalancing the bridge.

V. UNCERTAINTY

Tab. II reports, in addition to the estimated δ values, the associated uncertainties. These have been evaluated on the basis of the measurement model of Eq. (11); Tab. III and Tab. IV provide uncertainty budgets for the various configurations. The largest contributions to the uncertainty are related to the injection network of ΔV_H and to the measurement of ΔV_L performed with the synchronous detector. The uncertainty of ΔV_H can be reduced by improving the injection network, that is, by employing a digital source with higher resolution and

TABLE I
STANDARDS EMPLOYED FOR THE MEASUREMENTS. THE ASTERISK * DENOTES THE SECOND OF TWO STANDARDS HAVING THE SAME NOMINAL VALUE.

Label	Description
$100\,\Omega$	Agilent mod. 42036A: 10^{-3} tolerance, $\pm 10 \times 10^{-6}\,\mathrm{K}^{-1}$ temp. coefficient
*$100\,\Omega$	Vishay mod. VHA512 bulk metal foil precision resistor: 10^{-5} tolerance, $\pm 0.6 \times 10^{-6}\,\mathrm{K}^{-1}$ temp. coefficient, four terminal-pair casing
$25\,\Omega$	Tinsley mod. 5685A ac-dc standard resistor: 2×10^{-5} tolerance, $\pm 2 \times 10^{-6}\,\mathrm{K}^{-1}$ temp. coefficient

TABLE II
MEASUREMENT RESULTS

Z_A	Z_B	W^nom	$\delta^\mathrm{ref} \times 10^6$	For $r_\mathrm{L} = 0\,\Omega$			For $r_\mathrm{L} = 10\,\Omega$		
				I_A	I_B	$\delta^0 \times 10^6$	I_A	I_B	$\delta^\mathrm{L} \times 10^6$
$100\,\Omega$	*$100\,\Omega$	1	$-267(2)$	$6.8\,\mathrm{mA}$	$6.8\,\mathrm{mA}$	$-265(6)$	$6.2\,\mathrm{mA}$	$6.2\,\mathrm{mA}$	$-264(6)$
$25\,\Omega$	*$100\,\Omega$	0.25	$-6(2)$	$6.6\,\mathrm{mA}$	$1.7\,\mathrm{mA}$	$19(11)$	$5.1\,\mathrm{mA}$	$1.3\,\mathrm{mA}$	$30(12)$

TABLE III
UNCERTAINTY BUDGET FOR THE $100\,\Omega : 100\,\Omega$ COMPARISON.

i	Quantity	For $r_\mathrm{L} = 0\,\Omega$			For $r_\mathrm{L} = 10\,\Omega$			Remarks
		x_i	$u(x_i)$	$u_i(\delta^0) \times 10^6$	x_i	$u(x_i)$	$u_i(\delta^\mathrm{L}) \times 10^6$	
1	$\mathrm{Re}\,\epsilon$	0	10^{-6}	1	0	10^{-6}	1	Calibration [12]
2	$\mathrm{Re}\,\Delta V_\mathrm{H}$	$-164.5\,\mathrm{\mu V}$	$3.8\,\mathrm{\mu V}$	5.6	$-140.0\,\mathrm{\mu V}$	$3.2\,\mathrm{\mu V}$	5.2	Source channel accuracy
3	$\mathrm{Re}\,\Delta V_\mathrm{L}$	$16.0\,\mathrm{\mu V}$	$0.6\,\mathrm{\mu V}$	0.9	$24.0\,\mathrm{\mu V}$	$0.6\,\mathrm{\mu V}$	1.0	Detector gain and noise
4	V_BH	$0.680\,\mathrm{V}$	$0.004\,\mathrm{V}$	1.5	$0.621\,\mathrm{V}$	$0.004\,\mathrm{V}$	1.5	Detector gain
	δ	-265.4		6.0	-264.1		5.6	RSS

TABLE IV
UNCERTAINTY BUDGET FOR THE $25\,\Omega : 100\,\Omega$ COMPARISON.

i	Quantity	For $r_\mathrm{L} = 0\,\Omega$			For $r_\mathrm{L} = 10\,\Omega$			Remarks
		x_i	$u(x_i)$	$u_i(\delta^0) \times 10^6$	x_i	$u(x_i)$	$u_i(\delta^\mathrm{L}) \times 10^6$	
1	$\mathrm{Re}\,\epsilon$	0	10^{-6}	1	0	10^{-6}	1	Calibration [12]
2	$\mathrm{Re}\,\Delta V_\mathrm{H}$	$49.9\,\mathrm{\mu V}$	$1.2\,\mathrm{\mu V}$	7.0	$38.9\,\mathrm{\mu V}$	$0.9\,\mathrm{\mu V}$	7.0	Source channel accuracy
3	$\mathrm{Re}\,\Delta V_\mathrm{L}$	$46.8\,\mathrm{\mu V}$	$1.3\,\mathrm{\mu V}$	8.2	$35.0\,\mathrm{\mu V}$	$1.2\,\mathrm{\mu V}$	9.5	Detector gain and noise
4	V_BH	$0.165\,\mathrm{V}$	$0.001\,\mathrm{V}$	0.1	$0.128\,\mathrm{V}$	$0.001\,\mathrm{V}$	0.2	Detector gain
	δ	18.8		10.8	30.1		11.8	RSS

accuracy, and tailored voltage transformers with more suitable scaling ratios. The uncertainty of the present digital source has been considered in Tab. III and IV. The uncertainty of ΔV_L can be reduced by employing a compensation technique [3, Sec. 4.6.4.2] which, however, requires a source with additional output channels and injection transformers.

VI. DISCUSSION AND CONCLUSION

The results given in Tab. II show that the self-compensation functionality of the proposed bridge topology is highly effective. Consider e.g. the $25\,\Omega{:}100\,\Omega$ comparison. The insertion of r_L generates an additional voltage drop of about $51\,\mathrm{mV}$, a large fraction ($40\,\%$) of V_BH.

The values of ΔV_L, reported in Tab. III and IV for the two cases $r_\mathrm{L} = 0$ and $r_\mathrm{L} = 10\,\Omega$, differ only of a few $\mathrm{\mu V}$; it can be concluded that the rejection ratio of the voltage drops caused by lead impedances is the order of thousands or greater. Such self-compensation capability, at variance with full-compensation or combining network strategies, does not require any adjustment and is continuously operating, therefore

rejecting also any change in the impedance of the current paths (caused, for example, by drifts in contact resistances).

In a bridge employing a full-compensation strategy, like those described in Refs. [12], [13], this voltage drop has to be compensated with a countervoltage injection. The voltage generator which provides the injection has to be adjusted with a resolution, and a short-term stability (between two successive balances), comparable to the measurement accuracy.

It is possible to combine different strategies to achieve four terminal-pair impedance definition. For example, Ref. [24] improves the four terminal-pair voltage bridge of Ref. [25] by adding an active compensation to a combining network strategy.

It can be expected that the combination of the self-compensation topology here proposed with active compensation methods for 4TP impedance definition already extensively tested, either analogue [26] or digital [12], will allow an extension of the bridge impedance range well below $1\,\Omega$ maintaining accuracies of the order of 10^{-6} at audio frequency.

VII. Acknowledgments

References

[1] B. P. Kibble and G. H. Rayner, *Coaxial ac bridges*. Bristol, UK: Adam Hilger Ltd, 1984.

[2] S. Awan, B. Kibble, and J. Schurr, *Coaxial Electrical Circuits for Interference-Free Measurements*, ser. IET Electrical Measurement. Institute of Engineering and Technology, 2010.

[3] L. Callegaro, *Electrical impedance: principles, measurement, and applications*, ser. in Sensors. Boca Raton, FL, USA: CRC press: Taylor & Francis, 2013.

[4] N. L. Kusters, "The precise measurement of current ratios," *IEEE Trans. Instr. Meas.*, vol. 13, pp. 197–209, 1964.

[5] N. L. Kusters and W. J. M. Moore, "The development and performance of current comparators for audio frequencies," *IEEE Trans. Instr. Meas,*, vol. 14, pp. 178 –190, 1965.

[6] N. Kusters, "Current comparators — a new class of transformer-like devices," *Electronics and Power*, vol. 14, pp. 210–212, 1968.

[7] W. J. M. Moore and P. N. Miljanic, *The current comparator*, ser. IEE Electrical Measurement. London, UK: Peter Peregrinus Ltd, 1988, vol. 4.

[8] C. A. Desoer and E. S. Kuh, *Basic circuit theory*. McGraw-Hill, 1988.

[9] R. D. Cutkosky, "Four-terminal-pair networks as precision admittance and impedance standards," *Commun. Electron.*, vol. 70, pp. 19–22, 1964.

[10] J. Melcher, J. Schurr, K. Pierz, J. Williams, S. Giblin, F. Cabiati, L. Callegaro, G. Marullo-Reedtz, C. Cassiago, B. Jeckelmann, B. Jeanneret, F. Overney, J. Bohacek, J. Riha, O. Power, J. Murray, M. Nunes, M. Lobo, and I. Godinho, "The European ACQHE project: modular system for the calibration of capacitance standards based on the quantum Hall effect," *IEEE Trans. Instrum. Meas.*, vol. 52, pp. 563–568, 2003.

[11] S. P. Giblin and J. M. Williams, "Automation of a coaxial bridge for calibration of AC resistors," *IEEE Trans. Instrum. Meas.*, vol. 56, pp. 373–377, 2007.

[12] B. Trinchera, V. D'Elia, and L. Callegaro, "A digitally assisted current comparator bridge for impedance scaling at audio frequencies," *IEEE Trans. Instr. Meas.*, vol. 62, pp. 1771–1775, 2013.

[13] F. Overney, F. Luond, and B. Jeanneret, "Digitally assisted coaxial bridge for automatic quantum Hall effect measurements at audio frequencies," in *Proc. Conf. Precis. Electromagn. Meas. (CPEM)*, Aug 2014, pp. 226–227.

[14] L. Callegaro, V. D'Elia, M. Ortolano, and F. Pourdanesh, "A three-arm current comparator bridge for impedance comparisons over the complex plane," *IEEE Trans. Instrum. Meas.*, vol. 64, pp. 1466–1471, 2015.

[15] J. Nissilä, K. Ojasalo, M. Kampik, J. Kaasalainen, V. Maisi, M. Casserly, F. Overney, A. Christensen, L. Callegaro, V. D'Elia, N. T. M. Tran, F. Pourdanesh, M. Ortolano, D. B. Kim, J. Penttilä, and L. Roschier, "A precise two-channel digitally synthesized AC voltage source for impedance metrology," in *Proc. Conf. Precis. Electromagn. Meas. (CPEM)*, Rio de Janeiro, Brazil, 24-29 Aug 2014.

[16] W. J. M. Moore and S. K. Basu, "A direct-reading current-comparator bridge for scaling four-terminal impedances at audio frequencies," *IEEE Trans. Instr. Meas.*, vol. 15, pp. 253–259, 1966.

[17] L. Callegaro, V. DElia, J. Kučera, M. Ortolano, F. Pourdanesh, and B. Trinchera, "Self-compensating networks for four terminal-pair impedance definition in current comparator bridges," in *Proc. of the 2015 IEEE International Instrumentation and Measurement Technology Conference (I2MTC 2015)*, Pisa, May 2015, pp. 1658–1661.

[18] K. W. Wagner, "Zur messung dielektrischer Verluste mit die wechselstrombrücke," *Elektronische Zeitschrift*, vol. 32, pp. 1001–1002, 1911.

[19] B. Trinchera, L. Callegaro, and V. D'Elia, "Quadrature bridge for R–C comparisons based on polyphase digital synthesis," *IEEE Trans. Instr. Meas.*, vol. 58, pp. 202–206, 2009.

[20] L. Callegaro, V. D'Elia, and B. Trinchera, "Realization of the farad from the dc quantum Hall effect with digitally assisted impedance bridges," *Metrologia*, vol. 47, p. 464, 2010.

[21] R. M. Stitt, "AC coupling instrumentation and difference amplifiers," Burr Brown Application Bulletin AB-008, 1990.

[22] L. Callegaro, "On strategies for automatic bridge balancing," *IEEE Trans. Instr. Meas.*, vol. 54, pp. 529–532, 2005.

[23] J. Kovac and J. Kučera, "A modular coaxial multiplexer with high isolation between channels," in *Proceedings of the XXI IMEKO World Congress*, Aug 30 - Sep 4 2015, in press.

[24] R. Hanke and G. Ramm, "Reduction of kelvin ratio arm errors in an AC double bridge using electronic control," *IEEE Trans. Instr. Meas.*, vol. 32, pp. 145–146, 1983.

[25] R. Hanke, "Precise kelvin double bridge for measuring dissipation factors and capacitances up to 1 F," *IEEE Trans. Instr. Meas.*, vol. 27, pp. 434–436, 1978.

[26] L. Callegaro and V. D'Elia, "Automatic compensation technique for alternating current metrology based on synchronous filtering," *Rev. Sci. Instrum.*, vol. 69, pp. 4238–4241, 1998.